

Strong-Phase-Object Nano-Worlds Online

P. Fraundorf,^{1, a)} Stephen Wedekind,¹ and Taylor Savage¹

Physics & Astronomy/Center for Nanoscience, U. Missouri-St. Louis (63121), St. Louis, MO, USA

(Dated: 26 April 2016)

Although general multi-slice calculations remain too slow, web-browsers on many platforms now make possible real-time single-slice (strong phase/amplitude object) simulation, with live image, diffraction, image power-spectrum, and darkfield-image modes, including specimen rotation e.g. for atomic-resolution images with specimens having several tens of thousands of atoms. Moreover, a wide range of qualitative phenomena emerge that include diffraction-contrast effects associated with thickness, orientation changes, and defect strain. Hence students with no math background can get a visceral feel for the way 2-D lattice-projections, diffraction-patterns, image power-spectra, aperture size/position, and darkfield images relate to a specimen's structure & orientation, as well as microscope contrast-transfer, well before access to a real electron microscope is available.

CONTENTS

I. Introduction	1
II. Materials & Methods	1
III. Strong-phase-object simulation	2
IV. Nano-worlds on-line	2
A. Electron diffraction-pattern	2
B. Electron-optical image	3
C. Image power-spectrum	3
D. Digital darkfield image	3
V. Sample exercises	4
VI. Discussion	5
Acknowledgments	6

I. INTRODUCTION

Artifacts from specimen-preparation aside, transmission electron-microscopy (TEM) involves the effective use of electron-optics *plus* an understanding of beam-specimen interactions as well as insight into the structure of your particular specimen. Computer support for these characterization tasks is also evolving rapidly. However instrument-time for both operator-training and interface-development is limited and quite expensive.

In this note we discuss the potential of strong phase/amplitude-object simulations, with help from JavaScript (JS) on modern (HyperText Markup Language or HTML version 5) devices, to serve up an on-line, mobile-friendly platform for TEM operator-training and analytical TEM software-interface development. The simulator that we make available has already been put to

use with students in two NanoScience Practicals classes, and makes available real-time digital-darkfield tools useful with both deBroglie phase-contrast (e.g. high-resolution TEM) and incoherent amplitude-contrast (e.g. high-angle annular-darkfield scanning TEM or HAADF-STEM) lattice-images.

A surprising range of contrast-mechanisms (like thickness-fringes) manifest themselves (phenomenologically at least) without the need for slower multi-slice calculations. Microscopy-community ideas for new “unknowns” to add, as well as new analytical-features for the software interface, are invited in this context.

II. MATERIALS & METHODS

The first web-based real-time electron-image focus and astigmatism simulator involved pre-calculated images because personal computers in the 1990's were not yet able to do image-sized digital Fourier transforms at real-time speeds. However with today's processors, the speed of Javascript implemented in HTML5-canvas on a variety of browser platforms (including mobile devices) allows almost real-time implementation of the Cooley-Tukey FFT algorithm on e.g. 256×256 images. Our base simulators are presently hosted in University of Missouri - Saint Louis web-space, and they allow you to cycle through a handful of “unknowns” without having to refocus.

It is easy to create alternate instances with different specimens available. Versions of the application are under development which will allow specimen translation, procedural specimen-generation, and (eventually) field of view zooming as well.

We anticipate that users will become attached to specific specimen-collections e.g. for training purposes, so we plan to keep earlier collections available in a library as others become available. The left-hand pane located at <https://sites.google.com/site/electrondetectives> introduces and links to current versions of this web-browser application.

^{a)}Electronic mail: pfraundorf@umsl.edu

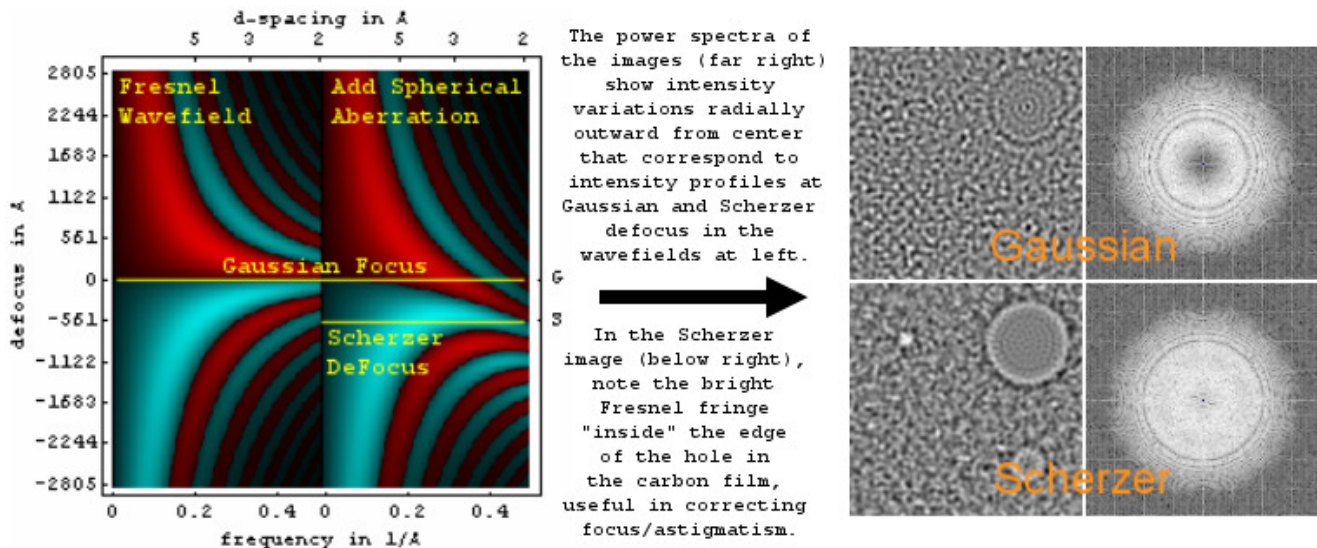


FIG. 1. Electron phase contrast transfer function and wavefield image analysis: At left find maps of contrast-transfer versus spatial-frequency without (left-half) and with (right-half) spherical aberration, as a function of imaging-system defocus in the vertical direction. At right find images (left-half) and image power-spectra (right-half) showing contrast transfer zeros at Gaussian and Scherzer defocus. In the thin-specimen limit, cyan bands (color on-line) in the panel at left show specimen-regions of increased projected-potential as darker, while red bands show contrast as reversed.

III. STRONG-PHASE-OBJECT SIMULATION

Because individual quanta in a nano-Ampere beam of 100 [keV] electrons are about an inch apart in the direction of travel, and because they unlike photons avoid the kind of shared-state coherence that we see in LASERS, individual electrons are the source of coherence (or its lack) in electron microscopy. However since electron-wavelengths shrink in the neighborhood of atomic-nuclei, each electron's wavefront experiences both phase and amplitude modulation as it passes through and between columns of atoms in a specimen.

Thus for electron phase-contrast imaging in a high-resolution TEM, for example, quantum-mechanics predicts an exit-surface deBroglie phase-lag, which varies with the projected-potential of atoms along the electron-trajectory¹⁻³. Fortunately, electron optics⁴ lets us convert this phase lag into an "intensity" map of projected-potential, at least across the transverse coherence-width of an electron's wave-packet. Unfortunately, multiple scattering alters quantitative interpretation of this map for specimens only a few light-atoms in thickness.

The good news, however, is that simulation of this phase-lag analysis can be used to qualitatively illustrate a wide range of electron contrast mechanisms. For instance, diffraction-contrast thickness-fringes along with the periodicity phase-inversions shown experimentally in Fig. 2 are included at least phenomenologically. Moreover, the same mathematics may be rather simply modified to yield amplitude-contrast maps (e.g. from incoherent-illumination darkfield-STEM) which are comparably robust.

IV. NANO-WORLDS ON-LINE

The phenomenological strengths of the strong-phase-object approximation, combined with the speed of fast-Fourier-transform (FFT) algorithms implemented in JavaScript on modern processors, gives one an ability to simulate online (in almost real-time, depending on processor speed) the exploration of nanomaterials with high energy electrons. By way of example, the 256×256 simulator that we have online⁵ provides the user with 4 panels, illustrated for example in the left half of Fig. 3.

A. Electron diffraction-pattern

We discuss the electron-diffraction pattern in the top-right panel first because in this case it is found "upstream" in the electron wave-field as (to first order) the log-intensity power-spectrum of the specimen's projected-potential. This assumes that we have managed to record it under parallel illumination conditions directly in the back-focal plane of the objective lens, without worry e.g. about lens aberrations. Microscopists might, in this context, think of it as a parallel-illumination selected-area diffraction-pattern of the region of the specimen in the field of view.

The electron diffraction-pattern (and to some extent the image power-spectrum below it) may be seen as a map of electron intensity as a function of scattering angle, as well as a map of specimen-region projected spatial-frequencies (increasing outward from the "DC-peak" or "unscattered-beam" at center). Although these panels

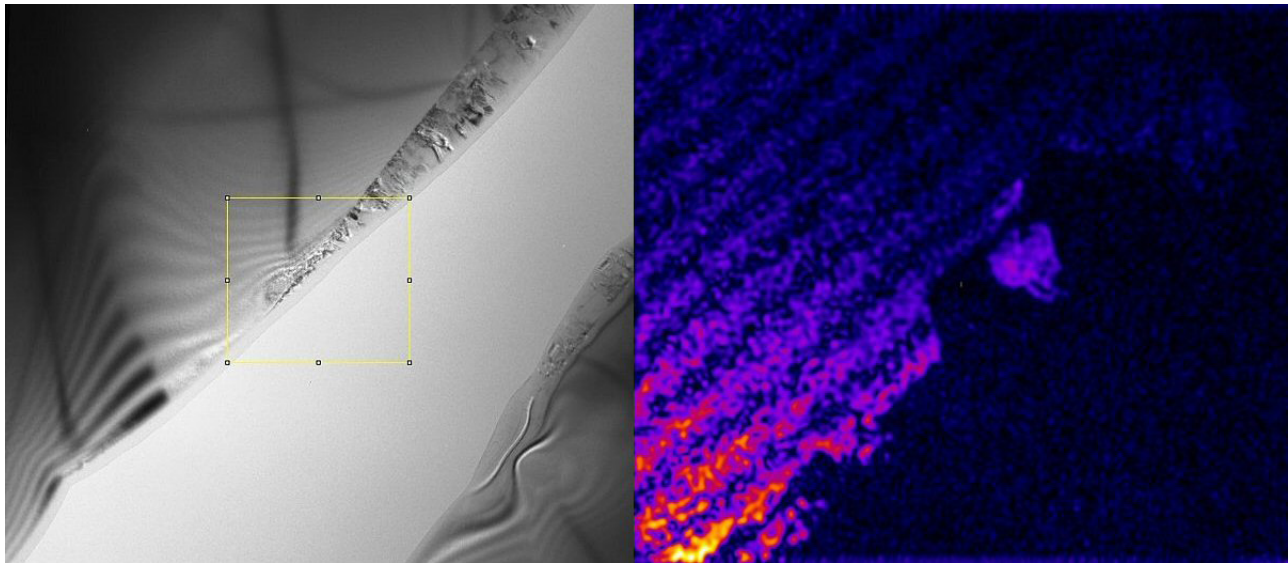


FIG. 2. Cross-section TEM image of poly-Si/Si (left), with a 111-fringe digital-darkfield amplitude-image (right) showing phase-inversion zeros twice per thickness-fringe, which also show up in strong-phase-object simulations.

do not contain “Fourier-phase information” which locates periodicities within the image, a great deal of information about possible candidate crystal structures in 2D (and after tilting in 3D^{6–17}) is available from these patterns.

An added advantage of high-energy electron diffraction-patterns is that the small size of the electron wavelength means that experimental patterns represent planar (i.e. flat Ewald-sphere) slices through the scattering reciprocal-lattice of the specimen region. Real-time tilting therefore should let operators imagine that they are “lighting up” a planar-slice through a three-dimensional structure whose inverse transform is the specimen itself.

B. Electron-optical image

The centerpiece of the simulator (from which later panels are obtained) is the electron-optical image in the top-left panel, which is of course recorded “downstream” of the microscope’s imaging lenses. This is affected by the microscope’s damping envelope and spherical aberration coefficient (presently fixed), as well as by lens focus-settings which are adjustable with buttons above the top row of panels. When the page is loaded, the focus setting of the system is randomized (in the same way for all “unknowns”), so that a (one-time) exercise in correcting astigmatism and optimizing focus may be needed.

All panels of course are affected by specimen orientation, which along with unknown choice and darkfield aperture size are selected with buttons below the top row of panels. In the “non-translating” version of our application, the tilts are patterned after a double-tilt goniometer which (unlike the real case) has unlimited tilt range and perfect eucentricity over both axes.

C. Image power-spectrum

The panel at bottom-right is next, as it is simply a (log-intensity) power-spectrum of the electron-optical image at top-left. It should be similar to the diffraction pattern above, except for the loss of high spatial-frequency information near the edges due to microscope instabilities, and the loss of selected bands of information elsewhere in the pattern due to spherical-aberration zeros in the microscope’s contrast-transfer function. These are actually quite useful for focus and astigmatism correction, as well as for understanding lens effects on the images.

This panel also contains the digital-darkfield aperture, which much like a physical aperture in the back-focal plane of the diffraction pattern, allows the operator to form a “digital-darkfield” image^{18–24} of selected spatial frequencies. The aperture location is adjusted by clicking on the image power-spectrum, while its size is adjusted in the button row above.

D. Digital darkfield image

The panel at bottom-left shows the digital-darkfield image selected by the aperture in the power-spectrum to its right. The difference between a digital-darkfield and an optical-darkfield image is that, although limited by contrast-transfer in the recorded image, the digital-darkfield image is complex-valued and contains Fourier-phase information in 2D which is not available in diffraction-patterns or image power spectra *per se*.

Hence this image is rendered in logarithmic complex-color. Gradients in the Fourier-phase (represented in the image by the pixel’s “hue”) provide information on periodicity strains^{25–28}, although at this point we are

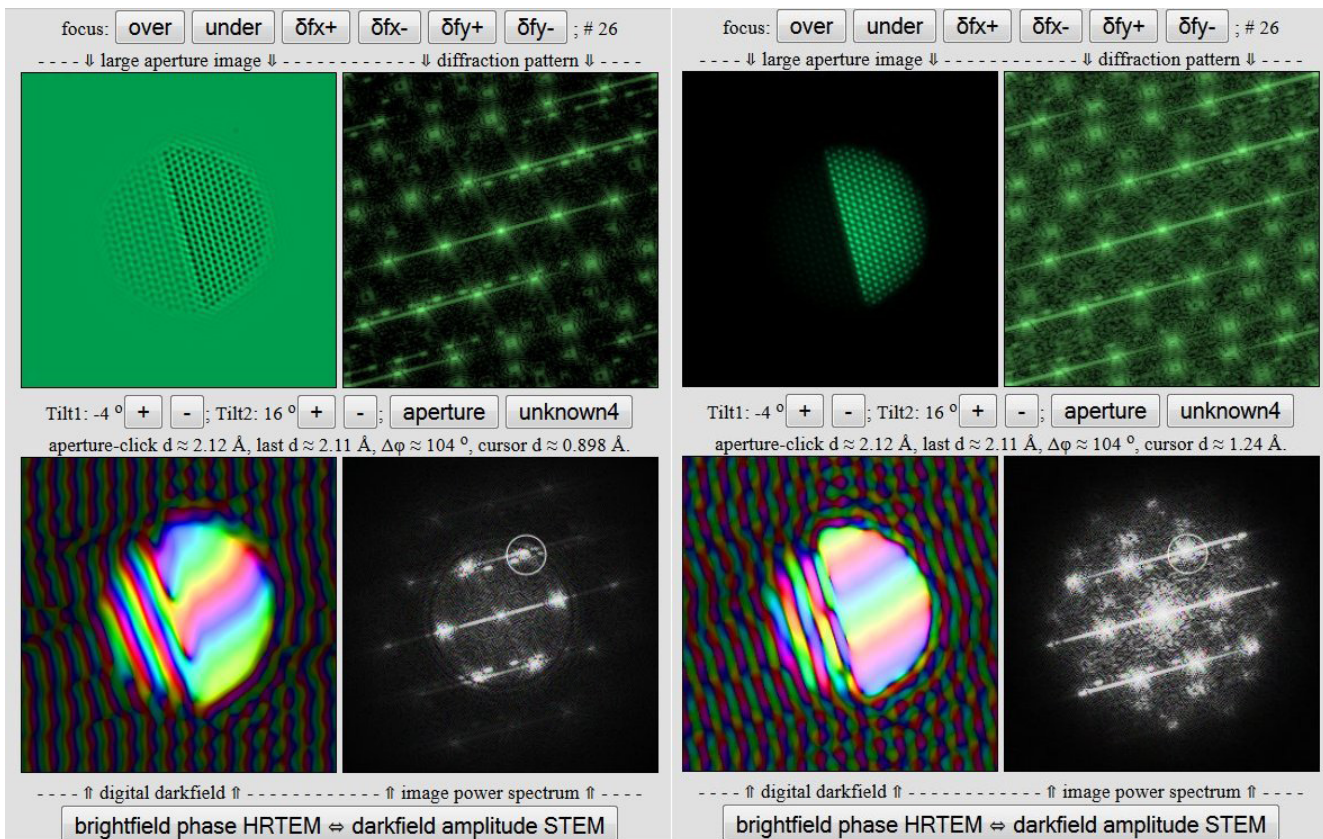


FIG. 3. Brightfield high-resolution TEM (phase) and darkfield scanning-TEM (amplitude) screenshots of an “unknown” specimen in an online simulator, with the same defocus, orientation, and darkfield-aperture.

not yet providing calculated vector strain-maps as well. Users of course will have the opportunity to interpret the strain-information from color variations across the digital-darkfield image itself, although this may take a bit of practice.

V. SAMPLE EXERCISES

In this section we mention some exercises (with the browser application mentioned above) for beginning students^{29,30} in two earlier NanoScience Practicals course implementations (with a third scheduled for Spring 2016). Observation exercises can be designed for students with only a general studies background, as well as for students already working on advanced characterization challenges. Perhaps the most remarkable result is the intuition that students develop about uses for a reciprocal-space (i.e. diffraction) aperture, before they get any field experience at all with a real microscope.

Correcting focus and astigmatism both with and without help from the image power spectrum: Initial practice without “counting adjustment-steps” in each case is recommended, just to see what is involved. It might then be interesting to report (on average) how many steps it takes for you (the student) to arrive at a

value satisfactory to you. In the “without help” case, an “exit-readout” also lists the defocus and astigmatism which which you end up. Averages for these might also be worth reporting.

Field width & magnification: Measure the width of the image panels on your device screen or printout to determine the magnification of the direct-space (left-side) images (of field-width $\simeq 11.3$ [nm]) as precisely as possible. Magnification may in turn be used to determine object sizes from the fact that X million (or Y thousand) times magnification means that a nanometer (or micron) on the object corresponds to X (or Y) millimeters in the image.

Size and shape analysis: Acquire data on the maximum and minimum projected widths (in \AA) of the unknown specimen in a single image and/or in three perpendicular directions, and from this estimate the specimen’s aspect-ratio, shape-category (i.e. equant, prolate, oblate or bladed), and average projected-area (in \AA^2) as well as (if possible) the unknown specimen’s surface-area (in cm^2) and volume (in cm^3),

Crystallinity: Take data on one or more characteristic-periodicities (in \AA) internal to the unknown specimen, and from this make a case for the number of single-crystal regions in the specimen (like that shown in Fig. 4) and hence on whether the speci-

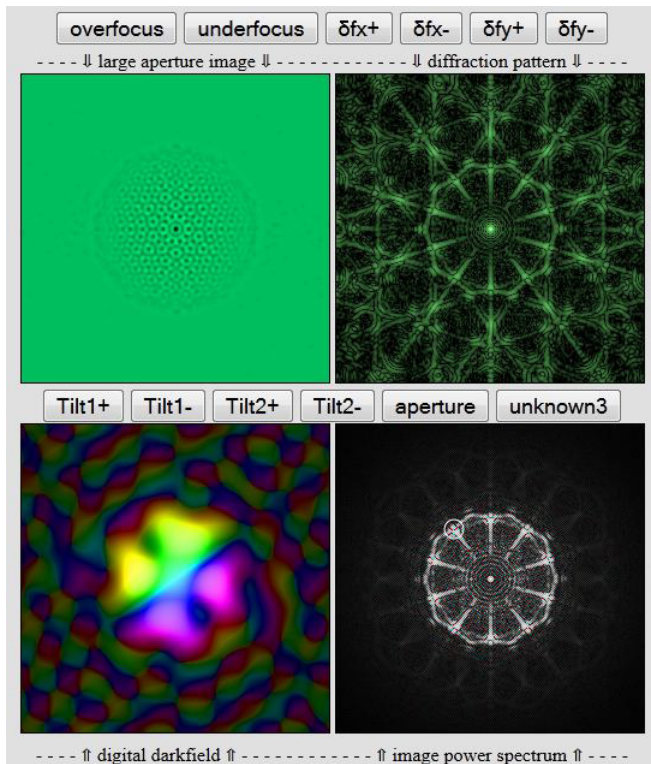


FIG. 4. Electron phase-contrast image of a 20-crystal icosahedral twin, seen down one of its 12 5-fold directions.

men is non-crystalline, poly-crystalline, bi-crystalline, or single-crystalline,

Candidate eliminations: If possible take “zone-axis-pattern” data from a single specimen-orientation on two lattice-spacings (e.g. in Å) associated with a single-crystal region of the unknown specimen, and on the angle (e.g. in degrees) between those periodicities. Diffraction is very powerful at saying NO. In other words periodicities not present in a particular crystal-structure, which e.g. “light up” our unknown crystal in a darkfield image, can rather strongly eliminate crystal-structure candidates (like those mentioned in the proposed specimen list above) from consideration. This webpage³¹ may help check your “two-spacing one-angle” measurements against some common candidates. Which structures can your observations rule out?

Crystal-lattice identification (e.g. 2D-spots): Given “zone-axis pattern” data (e.g. two lattice-spacings and the angle between them) from one single-crystal region of an unknown specimen, find a candidate crystal-structure that might be used to Miller-index the periodicities in the pattern. From this also calculate a possible lattice-direction $\langle uvw \rangle$ in that candidate-structure for the beam orientation itself,

More advanced techniques (e.g. 3D-spots, thickness, strain): For instance, take data on three (or more) non-coplanar lattice-spacings (in Å) in one (or all) single-crystal-region(s) of the unknown specimen,

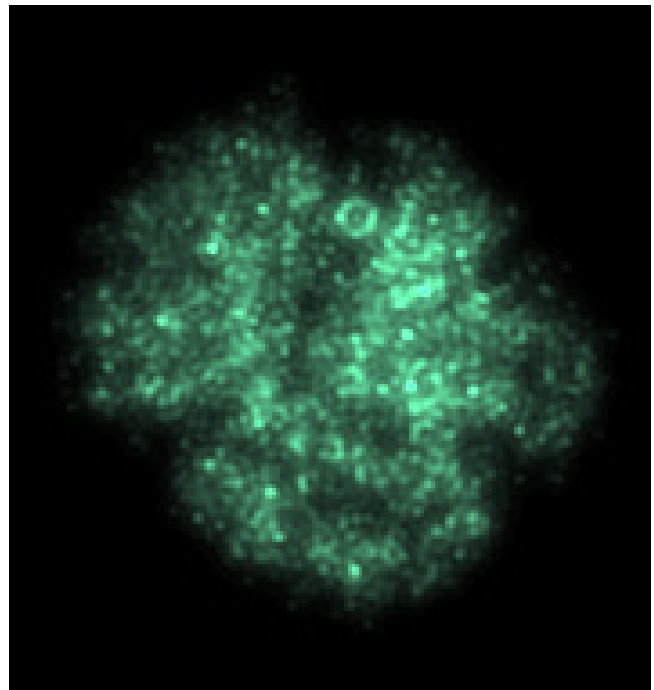


FIG. 5. Simulated HAADF image of a hemoglobin molecule in an on-line simulator, with a likely alpha-helix (circle at top) viewed end on in the absence of the vacuum re-arrangement, beam damage, and the need for a “support” that would be encountered experimentally.

and on the angles (in degrees) between the corresponding lattice-spacing g -vectors. From this data, determine lattice-parameters (a, b, c, α, β & γ) for the whole (or part) of the reciprocal-lattice of one (or all) of those single-crystal-regions, as well as the oriented-basis-triplet which defines that region’s orientation with respect to the specimen-stage.

VI. DISCUSSION

As discussed above, single-slice strong-phase-object electron diffraction and image simulations in nearly real-time are now available online through many devices that support a web browser. Students can already get some visceral experience with electron-diffraction and electron-imaging as it is used today, to provide insight into a wide range of condensed-matter challenges in the physical and life sciences. In the latter context Fig. 5 shows what the alpha-helix in a hemoglobin molecule might look like edge-on, if we can find a way to either average over or lessen the effects of vacuum and ionization damage in real electron microscopes.

A wide range of other interesting “nano-specimens” remain yet to be assembled. Suggestions for specimens that might help in your facility are invited in that context. In addition to specimen-tilting, future incarnations of these online simulators will allow for other imag-

ing and analysis modes, specimen translation, and even zooming from nanometer to millimeter field-widths on procedurally-generated specimens.

Today's microscopists and facility-managers, as well as their students, can help with these developments. These in turn will help with development of improved-interfaces to current and future instruments, with e.g. real-time digital-darkfield and lattice Fourier phase-gradient analysis, as well as analysis of periodicities seen in diffraction patterns and images taken at more than one tilt.

ACKNOWLEDGMENTS

PF implemented the first on-line TEM focus & astigmatism simulator in 1996³² using precalculated 128²-pixel images. SW catalyzed development of the JS/HTML5-canvas version discussed here, while TS assembled some unknown atom-position lists esp. of non-crystalline materials.

- ¹J. C. H. Spence, *Experimental high-resolution electron microscopy*, 2nd ed. (Oxford University Press, 1988).
- ²L. Reimer, *Transmission electron microscopy: Physics of image formation and microanalysis*, 4th ed. (Springer Science, NY, 1997).
- ³E. J. Kirkland, *Advanced Computing in Electron Microscopy*, 2nd ed. (Plenum Press, NY, 2010).
- ⁴O. Scherzer, "The theoretical resolution limit of the electron microscope," *J. Appl. Phys.* **20**, 20–29 (1949).
- ⁵P. Fraundorf, "Nanoworld explorer," Archived by WebCite at <http://www.webcitation.org/6f3MFIW4x> (2014).
- ⁶P. Fraundorf, "Stereo analysis of single crystal electron diffraction data," *Ultramicroscopy* **6**, 227–236 (1981).
- ⁷P. Fraundorf, "Stereo analysis of electron diffraction patterns from knowns," *Ultramicroscopy* **7**, 203–206 (1981).
- ⁸P. Fraundorf, "Determining the 3D lattice parameters of nanometer-sized crystals from images," *Ultramicroscopy* **22**, 225 (1987).
- ⁹W. Qin, *Crystal lattice parameters from direct-space images at two tilts*, Ph.D. thesis, Physics and Astronomy University of Missouri Saint Louis (2000).
- ¹⁰W. Qin and P. Fraundorf, "Lattice parameters from direct-space images at two tilts," *Ultramicroscopy* **94**, 246–262 (2003).
- ¹¹P. Fraundorf, W. Qin, P. Moeck, and E. Mandell, "Making sense of nanocrystal lattice fringes," *J. Appl. Phys.* **98**, 114308 (2005).
- ¹²P. Wang, A. L. Bleloch, U. Falke, and P. J. Goodhew, "Geometric aspects of lattice contrast visibility in nanocrystalline materials using haadf stem," *Ultramicroscopy* **106**, 277–283 (2006).
- ¹³J. Wang and P. Fraundorf, "Lattice fringe signatures of epitaxy on nanotubes," *Microscopy and Microanalysis* **12**, 664–665 (2006).
- ¹⁴P. Moeck and P. Fraundorf, "Structural fingerprinting in the transmission electron microscope," *Zeitschrift fuer Kristallographie* **222**, 634–645 (2007).
- ¹⁵S. Mukherjee, B. Ramalingam, L. Griggs, S. Hamm, G. A. Baker, P. Fraundorf, S. Sengupta, and S. Gangopadhyay, "Ultrafine sputter-deposited pt nanoparticles for triiodide reduction in dye-sensitized solar cells: impact of nanoparticle size, crystallinity and surface coverage on catalytic activity," *Nanotechnology* **23**, 485405 (2013).
- ¹⁶S. Meyer and P. Fraundorf, "Geometry versus paint models of FCC lattice-fringe visibility," *Microscopy and Microanalysis* **19**, 804–805 (2013).
- ¹⁷P. Fraundorf, "Lattice-image estimates of nano-particle fraction crystalline," *Microscopy and Microanalysis* **19**, 1590–1591 (2013).
- ¹⁸P. Fraundorf and G. K. Fraundorf, "Fourier transform darkfield techniques," in *Proc. 47th Annual Meeting of the Electron Microscope Society of America* (San Francisco Press, CA, 1989) pp. 122–123.
- ¹⁹P. Fraundorf, "Digital darkfield decompositions," arXiv:cond-mat/0403017 [cond-mat.mtrl-sci] (2004).
- ²⁰P. Fraundorf and L. Fei, "Digital darkfield decompositions," *Microscopy and Microanalysis* **10**, 300–301 (2004).
- ²¹P. Fraundorf, J. Wang, E. Mandell, and M. Rose, "Digital darkfield tableaux," *Microscopy and Microanalysis* **12**, 1010–1011 (2006).
- ²²P. Fraundorf, J. Liu, and E. Mandell, "Digital darkfield analysis of nanoparticle defects," *Microscopy and Microanalysis* **13**, 992–993 (2007).
- ²³P. Fraundorf and C. Bishop, "Efficient lattice-image detection of icosahedral twin," *Microscopy and Microanalysis* **19**, 1804–1805 (2013).
- ²⁴P. Fraundorf, "Digital darkfield analysis of lattice fringe images with ImageJ," *Microscopy and Microanalysis* **20**, 824–825 (2014).
- ²⁵M. Takeda and J. Suzuki, "Crystallographic heterodyne phase detection for highly sensitive lattice distortion measurements," *J. Opt. Soc. Am. A* **13**, 1495–1500 (1996).
- ²⁶M. J. Hÿtch, "Analysis of variations in structure from high resolution electron microscope images by combining real space and Fourier space information," *Microsc. Microanal. Microstruct.* **8**, 41–57 (1997).
- ²⁷M. Rose, *Spacing measurement of lattice fringes in HRTEM images using digital darkfield decomposition*, Master's thesis, Physics and Astronomy University of Missouri St. Louis (2006).
- ²⁸M. Rose and P. Fraundorf, "Picometer scale differences of lattice spacing in TEM images," *Microscopy and Microanalysis* **12**, 1008–1009 (2006).
- ²⁹P. Fraundorf and N. Pongkrapan, "Students as nanodetectives in web-connected intro science classes," *Microscopy and Microanalysis* **10**, 1564–1565 (2004).
- ³⁰P. Fraundorf and K. Stine, "Nanoworld webquests with peer review," *Microscopy and Microanalysis* **12**, 1700–1701 (2006).
- ³¹P. Fraundorf, "Two-spot indexing-laboratory v1.0 at UM-StL," Archived by WebCite at <http://www.webcitation.org/6f4hHby88> (2011).
- ³²P. Fraundorf, "Interactive focus and astigmatism adventures on the web," Archived by WebCite at <http://www.webcitation.org/6f1kEhUC2> (1996).